

## EUTROPHICATION MODELLING FOR SINGAPORE WATERS

**P. SUNDARAMBAL AND P.TKALICH\***

*Tropical Marine science Institute, National University of Singapore*

\* *tmspt@nus.edu.sg*

### Introduction

Singapore is a tropical country situated between latitudes 1°06'N and 1°24'N and longitudes 103°24'E and 104°24'E, 137 km north of the equator (Figure 1). The Republic is located to the south of Peninsular Malaysia and is separated from its northern neighbour by Johor Straits. To the south are scattered the islands of the Indonesian Riau archipelago. The coastal water of Singapore is bounded by the Johor Straits in the North and the Singapore Straits in the South. The Singapore Straits is a channel where three different water bodies meet: the Java Sea to the south, the South China Sea to the east and Malacca Straits to the Northwest. The hydrographical conditions of Singapore are dominated by the semi-diurnal tides and by the northeast and southwest monsoons. General climate features like temperature, rainfall and wind currents have remained somewhat consistent over the years, although some limited variations have occurred. In Singapore, significant coastal developments have arisen as a result of economic growth since the 1960s. Urbanisation of coastal zones often leads to increase of waste discharge into the aquatic environment. Organic and inorganic industrial waste, occasionally discharged into the coastal waters, can have acute and long-term impact on the marine environment. Singapore is well-served by six major sewage treatment works with a total capacity of about 917,000 m<sup>3</sup>/day (Khoo, 1991). Among significant pollutants entering the marine waters are nutrients, heavy metals, oil, anti-fouling agents and the ballast water.

The biogeochemical cycling of carbon and nutrients in marine systems is receiving added attention in recent years. The biological environment stress as a result of human interventions may be examined in relation to the distribution and level of nutrients and contaminants in the water column, the occurrence of algal blooms, the state of various habitats, biodiversity and ecosystems. Even though seawater has self purification capacity, the combined chronic effect of pollutant and nutrient load may cause outbreak of harmful algal bloom (the so called "red tides"), eutrophication and loss of natural habitat. Eutrophication can be defined as the process of changing the nutritional status of a given water body by increasing the nutrient resources. Effects due to eutrophication can be classified as initial (generation of greater biomass of plant material and

thus affect energy flow in the entire ecosystem) and secondary effects (reduction in the depth, reduce benthic plants, reduce available oxygen and also cause "red tides"). The eutrophication in coastal marine environments may depend on hydrodynamic phenomena such as advection, diffusion, vertical stratification, frontal dynamics and the mixing of water column. The salinity and temperature stratification results in a spatial separation of photosynthetic and mineralization processes which can lead to oxygen depletion of the lower layers of the water column. The daylight penetration is affected by cloudiness caused by concentrations of plankton, by suspended organic and inorganic material in coastal water. The greater growth of plants causes the greater amplitude of changes in dissolved oxygen and pH.

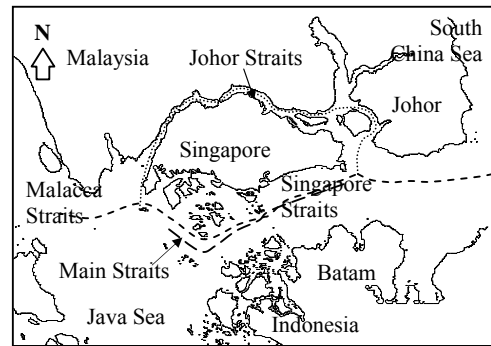


Figure 1. Singapore and its surrounding area

In South East Asia, the incidence of eutrophication of coastal waters has increased dramatically in recent years. Occurrences of harmful algal blooms have been reported in Hong Kong (Lam and Ho, 1989; Ho and Hodgkiss, 1995) and Philippines (Bajarias and Relox, 1996). In order to understand the long-term response of the coastal ecosystem to anthropogenic activities and to assess a threat of eutrophication of the coastal waters of Singapore, it is necessary to establish up-to-date baseline conditions of the physical, chemical and biological parameters in the coastal waters over a range of space and time scales. These data are important for quantification of the eutrophication processes and for proper management of marine ecosystems. Numerical models are becoming a common tool to predict the eutrophication level and to assist in the environmental impact assessment in coastal waters. A number of three-dimensional eutrophication models are available, such as CE-QUAL-ICM (Cercio and Cole, 1993), ERSEM and 2D MIKE21

EU (Baretta et al., 1994), HydroQual (1995), Ecological North Sea Model Hamburg (ECOHAM1) (Moll, 1997) and WASP6 (Ambrose et al., 2001) etc. for coastal waters. NEUTRO model (Gin and Tklich, 1998) was developed with the proficient kinetics of WASP model combined with the 3-D advection-diffusion contaminant transport module to account more accurately for the spatial and temporal ocean dynamics. For the tropical coastal water of Singapore this approach was later utilized by Cheong et al. (2000), Yun (2000) and Zhang (2000).

One of the earliest experimental efforts to understand the ecosystem in Singapore Straits was by Tham (1953). From 1996 to 1998, Gu (1998) and Gin et al. (2000) conducted field surveys of about 20 sampling stations in the Singapore Straits, from the east to the islands of the south-west coast of Singapore. These measurements are beneficial for understanding of the current state of the Singapore's coastal water. In order to predict phytoplankton and nutrient concentrations, which depend on depth variation of light and vertical structure of the water column, it is necessary to use a three-dimensional eutrophication model, coupling major physical, chemical and biological processes.

### Description of NEUTRO Model

#### Eutrophication Model Structure

The current version of eutrophication model NEUTRO (Tklich et al., 2002) predicts 3-D water quality dynamics with respect to nutrients, plankton, dissolved oxygen, bacteria and suspended solids. Seven interacting systems are involved, including the nitrogen, phosphorus, carbon and silica cycles; phytoplankton and zooplankton dynamics; and dissolved oxygen balance (Figure 2). The conceptual framework for the eutrophication kinetics in the water column is based on the WASP model.

The total of 13 state variables are considered as follows: Ammonia (NH<sub>3</sub>), Nitrate (NO<sub>3</sub>+NO<sub>2</sub>), Phosphate(PO<sub>4</sub>), Phytoplankton (PHYTO), Carbonaceous Biochemical Oxygen Demand (CBOD), Dissolved Oxygen (DO), Organic Nitrogen (ON), Organic Phosphorus (OP), Zooplankton, Bacteria, Total Suspended Solids (TSS), Available Dissolved Silica and Particulate Biogenic Silica.

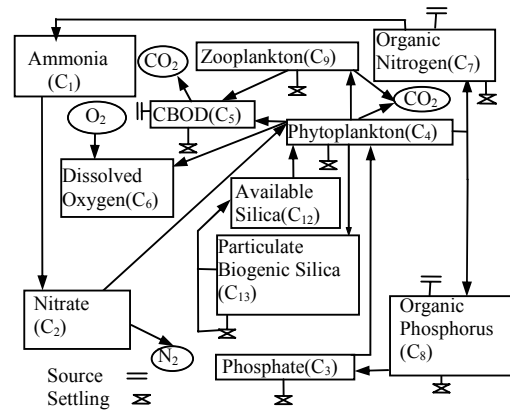


Figure 2. Sketch of nutrients, plankton and dissolved oxygen interaction

#### Nutrient Dynamics

Nitrogen is returned from phytoplankton biomass pool to the organic nitrogen pools as a result of phytoplankton death, endogenous respiration and zooplankton grazing and mortality. Organic nitrogen undergoes settling, hydrolysis, mineralization and a bacterial decomposition and the end product is ammonia at a temperature-dependent rate. Ammonia, in the presence of nitrifying bacteria and at a temperature- and oxygen- dependent rate, is then converted to (nitrification) nitrate. Denitrification occurs under anaerobic conditions and CBOD decreases due to stabilization. NH<sub>3</sub> and NO<sub>2</sub>+NO<sub>3</sub> are available for phytoplankton uptake, however, the preferred form is NH<sub>3</sub> for physiological reasons. But as NH<sub>3</sub> concentrations become depleted, phytoplankton will utilize NO<sub>3</sub> for growth. If nitrogen is limiting, the model also accounts for the preferential uptake of ammonia as compared to nitrate for phytoplankton growth kinetics (Thomann and Fitzpatrick, 1982). The ammonia preference is described by a factor P<sub>NH3</sub>.

$$P_{NH3} = \frac{C_1}{k_{mn} + C_2} \left( \frac{C_2}{k_{mn} + C_1} + \frac{k_{mn}}{C_1 + C_2} \right) \quad (1)$$

There is an adsorption-desorption interaction between dissolved inorganic phosphorus and dissolved particulate matter in the water column. The subsequent settling of suspended solids together with the sorbed inorganic phosphorus can act as significant loss mechanism in the water column and is a source of phosphorus to the sediment. The nutrient flux and death of phytoplankton produce organic nitrogen and organic phosphorus in the water column.

#### Plankton Dynamics

Phytoplankton, the group of free floating micro organisms, plays a critical role in coastal marine ecosystems because they are the major source of energy for higher tropic levels and for driving

nutrient cycles. Using light as energy source via photosynthesis, they produce organic compounds and oxygen by consuming inorganic nutrient. The phytoplankton growth relates to multiple factors, including available nutrients, water temperature, solar radiation, zooplankton grazing and tidal flushing. This model characterizes the aquatic plants as a whole by the total biomass of the phytoplankton present. So its maximum growth rate constant is adjusted throughout the simulation and is described as

$$G_p = f(\text{temperature, light, nutrients}) \quad (2)$$

It is assumed that phytoplankton population follows the Monod growth kinetics. Ambient light level is a function of time of day, depth and self-shading. Phytoplankton losses include endogenous respiration, mortality, exudation, settling, parasitization and grazing by herbivorous zooplankton. The zooplankton prey on phytoplankton as a food source, its grazing rate varies from species to species depending on (Di Toro et al., 1971) depending on temperature of water. Zooplankton kinetics depends primarily on grazing of phytoplankton and is reduced by mortality. As phytoplankton and zooplankton respire and die, biomass is recycled to nonliving organic and inorganic matter.

#### ***Dissolved Oxygen Balance***

In DO balance, five state variables namely phytoplankton carbon, ammonia, nitrate, carbonaceous biochemical oxygen demand, and dissolved oxygen play an important role. The sources of oxygen are atmospheric reaeration and phytoplankton photosynthesis. DO saturation depends on water salinity and temperature. The reaeration rate coefficient is a function of the average water velocity, depth, wind, and temperature. In NEUTRO model, a modification of Churchill et al.'s (1962) formulation is adopted as  $k_a = 5.049 V^{0.97} z^{-1.67} C_{\text{dofc}}$ , where  $k_a$  is the reaeration coefficient ( $\text{day}^{-1}$ ),  $V$  is the average flow velocity (m/s),  $z$  is the depth (m) and  $C_{\text{dofc}}$  is a dimensionless constant to fit the observed field data. The range of  $k_a$  values is 0.05/day and 12.2/day.

#### ***Total Suspended Solids and Fecal Coliform Bacteria Decay***

Total suspended solids are modelled as a non-reactive material, with a settling velocity similar to that of particulate organic matter. Once suspended, the solids originated from the man-made activities and photosynthetic process are transported and transformed by a number of different mechanisms. A portion of the organic solids will be lost by decomposition. The residual organic particles along with inorganic solids are subject to transport processes. The particles will be carried laterally by water currents. At the same time they will settle

differentially, depending on their size and density. Although a portion will remain permanently on the bottom, solids can be reintroduced into the water column by turbulence due to strong currents and in shallower areas due to wind mixing.

Pathogens are indicated in the model by faecal coliform bacteria, and the kinetics of bacterial die-off is modelled as a first order decay, with the rate constant ( $k_b$ ). Both, coliform bacteria and TSS are modelled as separate state variables, decoupled from the eutrophication parameters.

#### ***Silica***

Silica is very important state variable where diatoms biomass (40% of world phytoplankton) dominate ecosystem. Silica amounts limit the growth and behaviour of diatoms. The largest fluxes of silicate in the ocean's budget are driven by biological activity, potentially indicative of a system that can be biologically controlled. Because of their penchant for aggregation and sinking, it plays an important role in the biological pump of carbon to the deep ocean. High diatom cell counts observed in Johor Straits (Chia, 1988) when compared to Singapore Straits. They can be an indicator of water quality and pollution due to the ability to uptake and bind both organic and inorganic pollutants. The model incorporates two siliceous state variables, available silica and particulate biogenic silica. The silica cycle is a major biogeochemical cycle in which diatom takes up available silica and recycle available and particulate biogenic silica through the action of metabolism and predation. A portion of the settled particulate biogenic silica dissolves within the sediments and returns to the water column as available silica by mineralization. The silica kinetics is represented by diatom production and metabolism, predation, dissolution of particulate silica to dissolved silica which depends on alkalinity, settling and exchange rate.

#### **Governing equations and numerical methodology**

Mass transport and kinetic equations for dissolved constituents in a body of water must account for all materials entering and leaving through direct and diffuse loading; advective and dispersive transport; and physical, chemical, and biological transformation. Consider the coordinate system as  $x$ - and  $y$ - coordinates are in the horizontal plane, and the  $z$ - coordinate is in the vertical plane. The 3-D advective- diffusive- kinetic equation is described as follows:

$$\begin{aligned} \frac{\partial C_j}{\partial t} + \frac{\partial C_j U}{\partial x} + \frac{\partial C_j V}{\partial y} + \frac{\partial C_j (W - w_j)}{\partial z} - \\ - \frac{\partial}{\partial x} \left[ E_x \frac{\partial C_j}{\partial x} \right] - \frac{\partial}{\partial y} \left[ E_y \frac{\partial C_j}{\partial y} \right] - \\ - \frac{\partial}{\partial z} \left[ E_z \frac{\partial C_j}{\partial z} \right] = \frac{Q(S_j - C_j)}{\Delta h \Delta x \Delta y} + R_j \end{aligned} \quad (3)$$

where

$C_j$  = concentration of j-th pollutant;

$S_j$  = contamination of the liquid source with j-th pollutant;

$Q$  = discharge of the liquid source;

$R_j$  = chemical reaction terms, corresponding to the interaction equations for state variables (equations 4);

$E_x, E_y, E_z$  = turbulent eddy coefficients;

$\Delta x, \Delta y, \Delta z$  = computational grid sizes in x-, y-, and z- directions, respectively;

$\Delta h$  = thickness of water layer

$w_j$  = settling velocity of j-th pollutant;

$U, V, W$  = currents velocity in x-, y-, and z- directions, respectively.

The values of  $U, V, W, E_x, E_y$  and  $E_z$  are computed using the 3-D hydrodynamic model (Pang et al, 2003). The interactions of 13 state variables in terms of eutrophication kinetics are described mathematically by a set of equations as follows:

$$\frac{dC_1}{dt} = D_p a_{nc} (1 - f_{on}) C_4 + k_{71} \Theta_{71}^{T-20} C_7 \frac{C_4}{k_{mpc} + C_4}$$

$$- k_{12} \Theta_{12}^{T-20} C_1 \frac{C_6}{k_{nit} + C_6} - G_p a_{nc} P_{NH_3} C_4$$

$$\frac{dC_2}{dt} = k_{12} \Theta_{12}^{T-20} C_1 \frac{C_6}{k_{nit} + C_6} - G_p a_{nc} (1 - P_{NH_3}) x$$

$$x C_4 - k_{2d} \Theta_{2d}^{T-20} C_2 \frac{k_{NO_3}}{k_{NO_3} + C_6}$$

$$\frac{dC_3}{dt} = D_p a_{pc} (1 - f_{op}) C_4 + k_{83} \Theta_{83}^{T-20} C_8 \frac{C_4}{k_{mpc} + C_4}$$

$$- G_p a_{pc} C_4$$

$$\frac{dC_4}{dt} = (G_p - D_p) C_4$$

$$\frac{dC_5}{dt} = a_{oc} k_{1d} C_4 + a_{oc} k_9 \Theta_9^{T-20} C_9 - k_D \Theta_D^{T-20} C_5 x$$

$$x \frac{C_6}{k_{BOD} + C_6} - \frac{5}{4} \cdot \frac{32}{14} k_{2d} \Theta_{2d}^{T-20} C_2 \frac{k_{NO_3}}{k_{NO_3} + C_6}$$

$$\frac{dC_6}{dt} = k_a \Theta_a^{T-20} (C_{os} - C_6) +$$

$$+ G_p \left( \frac{32}{12} + \frac{64}{14} a_{nc} (1 - P_{NH_3}) \right) C_4 -$$

$$- k_D \Theta_D^{T-20} C_5 \frac{C_6}{k_{BOD} + C_6} - \quad (4)$$

$$- \frac{64}{14} k_{12} \Theta_{12}^{T-20} C_1 \frac{C_6}{k_{nit} + C_6} -$$

$$- \frac{32}{12} k_{1r} \Theta_{1r}^{T-20} C_4$$

$$\frac{dC_7}{dt} = D_p a_{nc} f_{on} C_4 - k_{71} \Theta_{71}^{T-20} C_7 \frac{C_4}{k_{mpc} + C_4}$$

$$\frac{dC_8}{dt} = D_p a_{pc} f_{op} C_4 - k_{83} \Theta_{83}^{T-20} C_8 \frac{C_4}{k_{mpc} + C_4}$$

$$\frac{dC_9}{dt} = (k_{1g} C_4 - k_9) \Theta_9^{T-20} C_9$$

$$\frac{dC_{10}}{dt} = -k_b \Theta_{10}^{T-20} C_{10}; \quad \frac{dC_{11}}{dt} = -T_{SS} C_{11}$$

$$\frac{dC_{12}}{dt} = c_{sc} (k_{fd} D_p - G_p) C_4 f_{dp} - a_{ex} (k_{dis} C_{12} - C_{13})$$

$$\frac{dC_{13}}{dt} = c_{sc} (1 - k_{fd}) D_p C_4 f_{dp} + a_{ex} (k_{dis} C_{12} - C_{13})$$

Here,  $G_p = k_{1c} X_{RT} X_{RI} X_{RN}$  is phytoplankton growth rate, where  $X_{RT} = \Theta_{1c}^{T-20}$  is the temperature adjustment factor,  $k_{1c}$  is maximum growth rate of phytoplankton at optimum light and nutrients.

Light intensity to which the phytoplankton is exposed is not uniformly at the optimum value in the natural environment. The light limitation factor,  $X_{RI}$ , allows for photosynthesis to increase with light levels up to some maximum, after which further increases in light results in photo inhibition. Modeling frameworks developed by Di Toro et al. (1971), extending upon a light curve analysis formulated by Steele (1962), account for both the effects of supersaturating light intensities and light attenuation through the water column. Parker (1974) has made further modifications by introducing more parameters to add more flexibility in fitting experimental data as

$$X_{RI} = \frac{X_i}{I_s} \cdot \exp \left( - \frac{X_i}{I_s} + 1 \right)^\beta \quad (5)$$

Here,

$$X_i = I_{as} I_s \exp(-K_e z) x_d;$$

$$K_e = K_e^0 + (0.0088 C_4 + 0.054 C_4^{0.67});$$

$\beta$  is a dimensionless constant as 0.1; and the ambient light levels are a function of length of a day as

$$x_d = \sin\left[\frac{2\pi}{86400}(t_h - t_{dl})\right]^3$$

and depth (Ikusima,1967).  $X_{RI}$  is the light limitation factor which is a function of average daily surface solar radiation  $I_{as}$ ; and saturating light intensity  $I_s$ ; daylight fraction of day  $f$ ; total light extinction coefficient  $K_e$ , (Riley, 1956) as the sum of the non-algal light attenuation  $K_e^0$  and the phytoplankton self-shading attenuation; depth  $z$ ; the hydrodynamic starting time  $t_h$  and the starting time of daylight  $t_{dl}$ .

The effect of nutrients on the growth of phytoplankton is quite complex. According to the Monod growth kinetics, the growth rate proceeds at the saturated rate for the ambient temperature and light condition. At low substrate concentration, however, the growth rate becomes linearly proportional to the substrate concentration. Thus, for a nutrient with concentration  $C_j$ , the factor by which the saturated growth rate is reduced is:  $C_j/(k_m+C_j)$ . The constant,  $k_m$  (called the Michaelis-Menten or half saturation constant) is the nutrient concentration at which the growth rate is half the saturated growth rate. If diatom is included in the model, then limiting factor for silica should also be considered in finding the nutrient limitation factor  $X_{RN}$  as a function of dissolved inorganic phosphorus and nitrogen, as

$$X_{RN} = \min\left\{\frac{C_1 + C_2}{k_{mn} + C_1 + C_2}, \frac{C_3}{k_{mp} + C_3}\right\}$$

$D_p = k_{lr}(T) + k_{ld} + k_{lg}$   $C_9$  is total biomass reduction rate of phytoplankton,  $k_{lr}(T)=k_{lr}(20^{\circ}C)\Theta_{lr}^{T-20}$  is endogenous respiration rate,  $k_{ld}$  is the death rate representing the effect of parasitization,  $k_{lg}$  is a grazing rate of phytoplankton per unit zooplankton population.

Settling rates of each state variable are important in their overall concentration reduction. Phytoplankton settling velocity ranges from about 0.1 to 0.3 m/day (Di Toro et al. 1971), and represents the net loss of phytoplankton through the bottom interface of water body. This net settling depends on phytoplankton species, time of day, and nutritional status of the plankton. Under quiescent flow conditions, the particulate fraction of CBOD can settle downward through the water column and deposit on the bottom. The deposition of CBOD can fuel sediment oxygen demand in benthic sediment. Particulate organic and inorganic phosphorus, particulate organic nitrogen, suspended solids and bacteria settle according to particulate fractions and user-specified velocities.

### Source Selection

Two alternative types of pollutant source may be prescribed at any point of the computational domain: the Dirichlet type,  $C\sim C_s$ , and the Neumann type,  $\partial C/\partial t\sim C_s$ . The first type sources are used to maintain observed field measurements of water contamination resulted from runoff and poorly identified sources. The second type is used when the characteristics of the effluent discharges are well known. The latter sources are applied for the outfall discharges from the Sewerage Treatment Works.

### Model Calibration

The model domain covers the main island of Singapore and its surrounding shelf waters, extending from approximately  $1^{\circ}0'N$  to  $1^{\circ}33'10.43''N$  (latitude) and from  $103^{\circ}20'E$  to  $104^{\circ}20'E$  (longitude). The model was run using two horizontal grids of 1 km and 0.5 km with 10 vertical layers at 0, 2.5, 5, 7.5, 10, 20, 40, 60, 80 and 120m. Simulations are typically run for a period of 10 to 30 days, using an automatically adjustable time step. Output results of the state variables are analyzed as time series at selected locations (Figure 3) or as spatial plots captured periodically. A majority of the kinetic coefficients were initially estimated from the Potomac Estuary Study (Thomann and Fitzpatrick, 1982). Each of the coefficients has a certain range that corresponds to a respective physical phenomenon. Within these ranges, the coefficient may vary according to local environmental conditions. The chosen values of the coefficients have to keep the state variables at quasi-steady (baseline) levels under the fixed nutrient load conditions. The fine-tuning may be done by solving Eq. (4) subject to the kinetic coefficients (Appendix 1). The periodic oscillations observed are due to a combination of the daily photosynthetic process and tidal forcing.

### Baseline Concentration

The baseline concentrations (Appendix 2) were obtained from field measurements in the Singapore seawaters. An extensive analysis is done for data processing and statistical analysis. The data more affected by local sources of pollution (Figure 4) are statistically filtered out, and the rest of data are analyzed to find the statistically mean baseline values by ANOM (ANalysis Of Mean) (Figure 5) with the Confidence Interval of 95% using a statistical software MINITAB (2000). Box plots tend to be most useful when there are many observations in the data set. The existing data set has many observations in each month at different monitoring stations. The observation is considered as outlier if it is different from the sample mean by more than twice the pooled standard deviation. The outlier measurements are identified using statistical box-plot (Figure 6). The baseline is set as initial

conditions for NEUTRO parameters. Iterative runs are performed to fine-tune the kinetic coefficients which provide the quasi-equilibrium response of the model. The 3-D tidal currents are computed by Pang et al (2003).

The value of Nitrate Nitrogen used in the model is the mean of the sum of observed nitrate and nitrite ( $\text{NO}_3 + \text{NO}_2$ ) values. The Carbonaceous Biochemical Oxygen Demand is the mean of observed Biochemical Oxygen Demand. The phytoplankton concentration is calculated from observed mean chlorophyll a concentration multiplied by Carbon:Chlorophyll 'a' ratio. The assumed Carbon:Chlorophyll 'a' ratio is 30 which may vary in a range of 20-50 (Ambrose et al. 2001). The concentration of Organic Nitrogen is obtained by subtracting the sum of mean values of Ammonia, Nitrate and Nitrite concentration from mean value of observed Total Nitrogen concentration. Similarly, the concentration of Organic Phosphorus is calculated by subtracting mean value of observed Phosphate from mean value of observed Total Phosphorus. The phytoplankton parameters such as incident solar radiation and light extinction coefficient, salinity, temperature, dissolved oxygen are taken from field monitoring data. The extinction coefficient and average solar radiation in NEUTRO model is obtained from measured light extinction coefficients and incoming solar radiation respectively (Jayaraman, 2000).

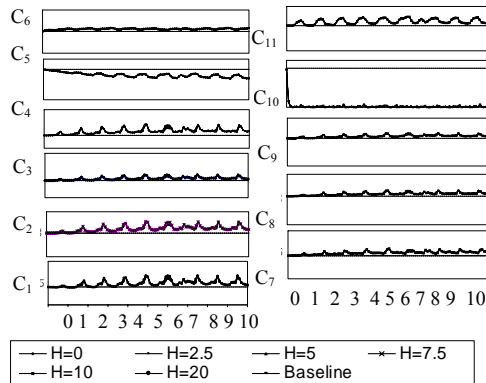


Figure 3. Model simulation results for baseline concentration at a monitoring station on the south coast of Singapore

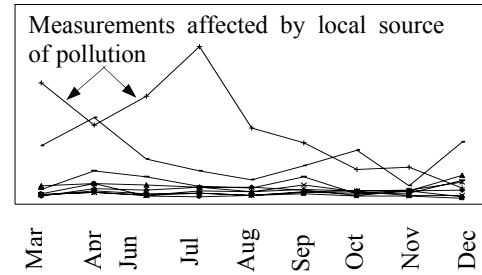


Figure 4. Selection of data stations for finding baseline parameter

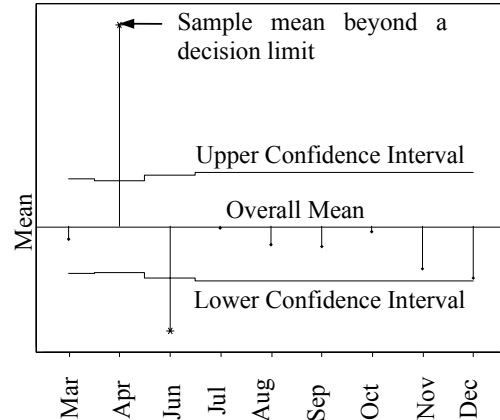


Figure 5. Statistical Mean value by ANOM (Analysis Of Mean)

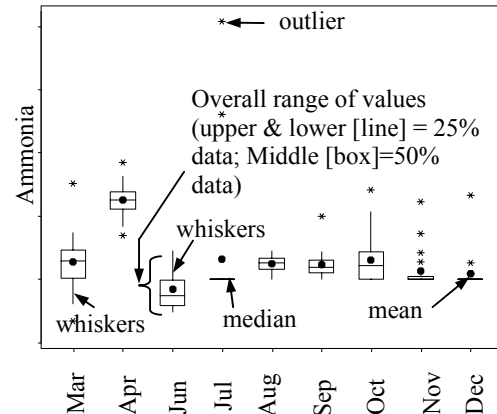


Figure 6. Mean value of Ammonia by Box Plot

### Conclusions

The three-dimensional eutrophication model NEUTRO for a tropical water column can be used for Environmental Impact Assessment in Singapore seawaters. Simulations using NEUTRO model show that the model output is achieving baseline levels, and is able to reproduce correctly general features and observed fine patterns in the water column of Singapore seawaters. More extensive calibration tuning is done to reproduce field monitoring data and day light effect for phytoplankton. The ability of the model to predict the fate and transport of nutrients, plankton,

suspended solids and bacteria, makes it useful in the study of environmental impact from coastal developments and outfall discharges. The model can be used to assist in the management and protection of Singapore's seawater and the surrounding region.

#### **Acknowledgements**

The authors would like to thank Prof. Chan, E.S, Assoc. Prof. Gin, K.Y.H. and Dr. M. Holmes for their helpful comments and suggestions; MPA Department and TMSI field monitoring group for providing data; A\*Star for providing funds, and to all TMSI staff who helped in this research work.

#### **References**

Ambrose B., Wool T.A. and Martin J.L. (2001) The Water quality Analysis Simulation Program. WASP6, User Manual, US EPA, Athens, GA.

Bajarias F.F.A. and Relox J.R. (1996) Hydrological and climatological parameters associated with the Pyrodinium blooms in Manila Bay, Philippines. In Yasumoto T., Oshima Y. and Fukuyo Y., Ed., Harmful and Toxic Algal Blooms, Intergovernmental Oceanographic Commission (IOC) of UNESCO, Paris, pp.49-52.

Baretta J.W., Ruardij P., Vested H.J. and Baretta-Bekker J.G. (1994) Eutrophication modeling of the North Sea: two different approaches. *Ecological Modeling*, 75/76, pp. 471-483.

Cerco C.F. and Cole T. (1993) Three-dimensional eutrophication model of Chesapeake, Bay. *Journal of Environmental Engineering*, 119, p. 1007.

Chia L.S., Habibullah K. and Chou L.M. (1988) Coastal environmental profile of Singapore. International Centre for living Aquatic Resources Management, Technical Publication series.

Cheong H.F., Shankar N.J., Ong C.E. and Huda M.K. (2000) Baseline study of water quality in Singapore coastal waters. Proceedings of XXIX IAHR Congress, Beijing, China, 2001.

Churchill M.A., Elmore H.L. and Buckingham R.A. (1962) Prediction of stream reaeration rates. *Journal of Sanitary Engineering Division, American Society of Civil Engineers*, SA4:1, Proceeding paper, p. 3199.

Di Toro D.M., O'Connor D.J. and Thomann R.V. (1971) A Dynamic model of the phytoplankton, population in the sacramento-san Joaguin Delta. *Advances in chemistry, American Chemical society*, 106, pp. 131-180.

Gin K.Y.H., Lin X. and Zhang S. (2000) Dynamics and size structure of phytoplankton in the coastal waters of Singapore. *Journal of Plankton research*, 22(8), pp. 1465-1484.

Gin K.Y.H. and Tkalich P. (1998) A three-dimensional eutrophication model for Singapore coastal water. Conference Proceedings of

Environmental Strategies for the 21st century, an Asia Pacific Conference, pp. 280-286.

Gu G. (1998) Phytoplankton dynamics in Singapore's coastal waters. M.Engg. Thesis, Department of Civil Engineering, National University of Singapore.

Ho K.C. and Hodgkiss I.J. (1995) A study of red tides caused by *Prorocentrum* spp. Ehrenberg, P. *Sigmoides* Bohm and P. *Triestinum* Schiller in Hong Kong. In Morton B., Hu G., Zou R., Pan J. and Cai G. Ed., *The Marine Biology of the South China sea II*. World Publishing Corporation, Beijing, PRC, pp.111-118.

HydroQual, Inc. and Normandeau Associates, Inc. (1995), A water quality model for Massachusetts and Cape Cod Bays: Calibration of the Bays Eutrophication Model (BEM). Research Report, Massachusetts Water resource Authority, Boston, Massachusetts.

Ikusima I. (1967) Ecological studies on the productivity of aquatic plant communities. III. Effect of depth on daily photosynthesis in submerged macrophytes. *Botanical Magazine*, Tokyo, 80, pp. 57-67.

Jayaraman V. (2000) Sediment nutrient flux along the coastal areas of Singapore. M. Engg. thesis, Department of Civil Engineering, National University of Singapore.

Khoo C.H. (1991) Land based sources of pollution in the coastal waters of Singapore. In Chia L.H. and Chou L.M., Ed., *Urban coastal area management: the experience of Singapore*. ICLARM Conference Proceedings 25, International Centre for Living Aquatic Resources Management, Philippines, pp. 77-80.

Lam C.W.Y. and Ho K.C. (1989) Red tides in Tolo Harbour, Hong Kong. In Okaichi, T., Anderson, D.M. and Nemoto, Ed., *Red Tides: Biology, Environmental Science and Toxicology*, Elsevier, New York, Amsterdam, London, pp.49-52.

Moll A. (1997) Modeling primary production in the North Sea. *Oceanography*, 10, pp. 24-26.

MINITAB Release 13.2 (2000) Minitab Inc., 3081 Enterprise Drive, State College, PA, U.S.A., website: <http://www.minitab.com>.

Pang W.C., Tkalich P. and Chan E.S. (2003) Hydrodynamic forecast model for the Singapore Straits. Accepted for presentation at XXX IAHR Congress 24-29 August 2003, Greece.

Parker R. A. (1974) Empirical functions relating metabolic processes in aquatic systems to environmental variables. *Journal of fishery research board of Canada*, 31, pp. 1550-1552.

Steele J. H. (1962) Environmental control of photosynthesis in the sea. *Limnology and Oceanography*, 7(2), pp. 137-150.

Tham A.K. (1953) A preliminary study of the physical, chemical and biological characteristics of Singapore. Fishery Publication 1, 4, pp. 6-39.

Thomann R.V. and Mueller J.A. (1987) Principles of Surface Water Quality Modeling and Control. Harper & Row, Publishers, New York.

Thomann R.V. and Fitzpatrick J.J. (1982) Calibration and verification of a model of the Potomac Estuary, Final Report to D.C. Dept. of Environmental Services, Washington, D.C.

Tkalich P., Pang W.C. and Sundarambal P. (2002) Hydrodynamic and eutrophication modelling for Singapore Straits. Conference Proceedings of The Seventh OMISAR Workshop on Ocean Models for the APEC Region (WOM7), Singapore, pp. 5(1-9).

Zhang Q.Y. (2000) A three dimensional eutrophication model for Singapore coastal water, PhD thesis, Department of Civil Engineering, National University of Singapore, 192 pp.

Yun C.K. (2000) Eutrophication modeling and simulation using Stella software. M.Engg. Thesis, Department of Civil Engineering, National University of Singapore.

**Appendix 1. Verified kinetic coefficients and other parameters used in NEUTRO model**

$a_{nc}$ =Nitrogen/carbon ratio;  $f_{on}$ =Fraction of dead phytoplankton recycled to the organic nitrogen pool;  $a_{pc}$ =Phosphorus/carbon ratio;  $f_{op}$ =Fraction of dead phytoplankton recycled to the organic phosphorus pool;  $k_{71}$ =Organic nitrogen mineralization rate;  $k_{12}$ =Nitrification rate;  $k_{2d}$ =Denitrification rate;  $k_{83}$ =Organic phosphorus mineralization rate;  $f_{d3}$ =Fraction of dissolved inorganic phosphorus in water column;  $f_{d5}$ =Fraction of dissolved CBOD in water column;  $f_{d5}$ =Fraction of dissolved organic nitrogen in water column;  $f_{d8}$ =Fraction of dissolved organic phosphorus in water column;  $k_{1r}$ =Endogenous respiration rate @ 20C;  $k_{1c}$ =Max specific growth rate @ 20C;  $k_{mn}$ =Half-saturation constant for nitrogen uptake;  $k_{mp}$ =Half-saturation constant for phosphorus;  $k_{1d}$ =Death rate for phytoplankton;  $DB$ =Non-algal extinction coefficient;  $f$ =Fraction of day that is daytime;  $sol$ =solar radiation;  $I_s$ =saturating light intensity;  $k_{1g}$ =Grazing rate of zooplankton;  $k_9$ =Death rate for zooplankton;  $a_{oc}$ =Oxygen/carbon ratio;  $k_{NO_3}$ =Half-saturation constant for oxygen limitation of denitrification;  $k_{BOD}$ =oxidation;  $k_{mpc}$ =Half-saturation constant for phytoplankton limitation of phosphorus recycling;  $k_{nit}$ =half-saturation constant for oxygen limitation of nitrification;  $k_D$ =Deoxygenation rate for CBOD;  $C_{os}$ =Saturation concentration of dissolved oxygen;  $k_b$ =Bacteria decay rate;  $T_{SS}$ =Suspended solids decay rate;  $\Theta_{71}$ ,  $\Theta_{2d}$ ,  $\Theta_{83}$ ,  $\Theta_{1r}$ ,  $\Theta_{1c}$ ,  $\Theta_c$ ,  $\Theta_s$ ,  $\Theta_9$ ,  $\Theta_a$ ,  $\Theta_{10}$ =Temperature coefficients.  
Silica kinetic coefficients:

$c_{se}$ =Silica-Carbon ratio;  $k_{fd}$ =Fraction of diatom silica made available by predation ( $0 \leq k_{fa} \leq 1$ );  $f_{dp}$ =Percent of diatom in total phytoplankton;  $a_{ex}$ =Exchange coefficient of dissolved Si and particulate Si;  $k_{dis}$ =Partition coefficient of sorbed vs dissolved available silica ;  $k_{sil}$ =Half-saturation for  $Si(OH)_4$ .

**Appendix 2. Average baseline concentrations used as inputs into the model and to estimate kinetic coefficients**

symbol	Baseline concentration	Units
C <sub>1</sub>	0.0133	mg/L
C <sub>2</sub>	0.02	mg/L
C <sub>3</sub>	0.0116	mg/L
C <sub>4</sub>	0.01	mg C/L
C <sub>5</sub>	1.099	mg/L
C <sub>6</sub>	5.402	mg/L
C <sub>7</sub>	0.0796	mg/L
C <sub>8</sub>	0.0135	mg/L
C <sub>9</sub>	0.0279	mg C/L
C <sub>10</sub>	0.5	counts/100ml
C <sub>11</sub>	22.59	mg/L